

Article

Influence of SiO₂ on the Compressive Strength and Reduction-Melting of Pellets

He Guo, Xin Jiang *, Fengman Shen, Haiyan Zheng , Qiangjian Gao and Xin ZhangKey Laboratory for Ecological Metallurgy of Multimetallic Mineral (Ministry of Education),
Northeastern University, Shenyang 110819, China

* Correspondence: jiangx@smm.neu.edu.cn; Tel.: +86-189-0401-5206

Received: 10 July 2019; Accepted: 2 August 2019; Published: 3 August 2019



Abstract: The effects of SiO₂ content on the compressive strength, reduction behavior and melting-dripping properties of the pellets were investigated under experimental conditions. The experimental results indicated that the compressive strength of pellets gradually decreased with increasing SiO₂ content, mainly because the pellets with high SiO₂ had poor crystallization capacity, a more liquid phase and more pores. With increasing SiO₂ content from 2.19 wt% to 8.13 wt%, the reduction degree of pellets decreased due to the generation of 2FeO·SiO₂. Based on the morphology analysis, inside of the pellets, 2FeO·SiO₂ caused the compact structure and fewer microspores with increasing SiO₂ content, which was unfavorable for the reduction process and resulted in the decrease of the reduction degree. Also, increasing the SiO₂ content had negative effects on the melting-dripping properties of pellets. The melting-dripping properties can be improved by adding some sinter with high basicity in the mixed burden. The current work established the relation between SiO₂ content and reduction-melting behavior of pellets, which can provide theoretical and technical support for the effective utilization of pellets with different SiO₂ content in blast furnace process.

Keywords: SiO₂; pellet; compressive strength; reduction; melting behavior

1. Introduction

Iron-bearing materials should enable the reliable production of hot metal from a blast furnace (BF) or directly reduction iron (DRI) from a shaft furnace, particularly at minimum cost and at a large scale. Nowadays, acid pellets matching with high basicity sinters are main burden compositions of BF in China. Pellets are a kind of artificial iron ore and have many preferable metallurgical properties. For instance, the particle size of a pellet is relatively uniform, which is favorable for burden permeability in the BF; the pellet iron-grade is higher, which is favorable for effective iron content input in burden column and enhancing production efficiency; the reduction of pellets is easy, which is favorable for increasing gas utilization rate of BF, etc. Therefore, the consumption of pellets in BF is gradually increasing in many ironmaking plants by 20% in China and even in some BFs in Europe and North America. At present, many references had studied the metallurgical properties of pellets with different chemical compositions and categories [1–7].

Iljana et al. investigated the effect of adding limestone on the metallurgical properties of pellets, and found that the reducibility, swelling and cracking increased during the limestone was added into pellets. The main reason was that decomposed by limestone caused the increase of porosity of pellets [8]. Umadevi et al. studied the influence of basicity on iron ore pellet properties and microstructure. The reduction degradation index (RDI) of pellets first decreased and then increased with increasing basicity, because the structure of pellets changed during reduction [9]. Gao et al. found that the reduction swelling index (RSI) and compressive strength of reduced pellets increased with an increasing SiO₂ content. Reduction gas compositions could influence the formation of iron whisker,

and then impact RSI [10–12]. Dwarapudi et al. evaluated the effect of MgO and basicity on the quality and microstructure of pellets. They found that RDI and softening-melting characteristics improved with increasing basicity. Also, they found that adding MgO to acid pellets decreased considerably their swelling tendency [13,14]. In Mohanty's work, the effect of basicity on the reduction behavior of iron ore pellets was investigated; it was shown that the reduction rate decreased with increasing basicity due to the formation of calcium ferrite phases [15]. The compressive strength of pellets, an important property, indicated the capacity of pellets to cope with a load during their transport and storage and the load of burden materials in the blast furnace. Increasing Al_2O_3 content could hinder the diffusion of ions within a lattice and the growth of grains, which negatively influenced the oxidation of Fe_3O_4 and recrystallization of Fe_2O_3 [16–19]. Chen et al. investigated the reduction behavior of vanadium titano-magnetite pellet. They found that the diffusion-control step could be observably shortened via the decrease of pellet size [20]. The volume shrinkage of magnetite iron ore composite pellets was investigated during solid-state isothermal reduction, and then the reduction mechanism was further analysed. The shrinkage of composite pellet was mainly due to the weight loss of carbon and oxygen, sintering growth of gangue oxides and partial melting of gangue phase [21]. In order to obtain sufficient pellets strength, the induration process of oxidized pellets was an important procedure, containing the oxidation of magnetite phase and sintering of oxidized magnetite phase [22].

Based on the above literature, previous research has been conducted on the compressive strength, reduction behavior of pellets, including the effects of chemical composition and reduction condition on reduction properties. However, challenges still remain in the effects of SiO_2 and burden compositions on compressive strength and reduction-melting behavior. (1) One of the influence factors on the compressive strength is liquid phase amount. Most previous studies only focused on the compressive strength of different SiO_2 pellets, but ignored the generation of liquid phase amount. Therefore, the relation between liquid phase amount and compressive strength is necessary to better use the different SiO_2 content pellets, and also is one of the originalities of the present work; (2) Many researchers have investigated the effect of SiO_2 on reduction properties of pellets, but some key mechanisms are not yet clear. The SiO_2 can affect the fluidity of the liquid phase. Therefore, the distribution of $2\text{FeO}\cdot\text{SiO}_2$ between liquid phase and wustite is one of the key points to better understand the influence mechanism of SiO_2 , and also is the originality of the present work (3) The high temperature properties of different burden compositions was investigated in previous research, but the distribution of SiO_2 between metallic phase and slag phase is not yet clear, and this is part of the originality of the present work too.

With the intention of addressing these challenges, research was undertaken on the effect of SiO_2 on the compressive strength and reduction-melting properties of pellets requires elaboration, including (1) the compressive strength of pellets with different SiO_2 content, (2) the microstructure structure and phase composition of different SiO_2 pellets (the compressive strength mechanism), (3) the effect of SiO_2 on the reduction behavior and (4) the effect of SiO_2 and burden composition on melting-dripping of iron-bearing materials, (5) the relation between SiO_2 content and compressive strength, reduction-melting behavior will be built. The results can provide technical support for the use of pellets in BF.

2. Materials and Methods

2.1. Raw Materials

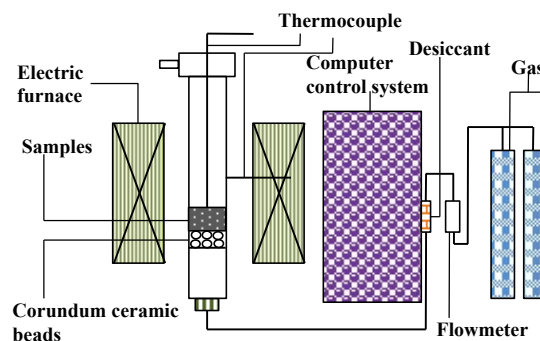
The raw material used in the study was obtained from the Hansteel Company (Handan, China). The chemical compositions of sinter and pellets are listed in Table 1. The raw materials included pellets and sinter, S denoted high basicity sinter and PA-PD denoted pellets with different SiO_2 contents. As can be seen in Table 1, the SiO_2 content in the pellets changed from 2.19 wt% to 8.13 wt%. In order to avoid experimental errors, the size of raw materials was uniform: sinter and pellets of 10–12 mm diameter were selected using the sieving method.

Table 1. Chemical compositions of the raw materials (wt%).

Samples	TFe	FeO	SiO ₂	CaO	MgO	Al ₂ O ₃	R (w(CaO)/w(SiO ₂))
S	57.74	8.55	5.02	9.65	1.79	1.94	1.92
PA	65.72	1.58	2.19	2.21	0.63	0.74	1.01
PB	65.73	0.83	4.63	0.66	0.34	0.34	0.14
PC	65.10	0.65	5.18	1.18	0.48	0.28	0.23
PD	63.81	0.00	8.13	0.31	0.49	0.43	0.04

2.2. Experiment Process

Figure 1 shows the experiment equipment for reduction property test, which it came from Northeastern University (Shenyang, China). The experimental set-up mainly included six components: a gas system, a desiccant, a computer system, a thermocouple, an electric furnace and a flowmeter. The inert atmosphere was maintained by blowing nitrogen gas and the reduction furnace was 800 mm in height and 75 mm in diameter. All reduction experiments were carried out using the reduction furnace. Before starting each experiment, the furnace was first heated to the target temperature (900 °C) in a nitrogen atmosphere, and then the pellets were placed into the constant temperature zone of the equipment. When the temperature was steady, the reduction gas (30%CO + 70%N₂) was introduced into the furnace at a total gas flow rate of 0.9 m³/h, and the reduction started. After a certain period of reaction time (3 h), the pellets were cooled in the furnace under 0.3 m³/h N₂ to ambient temperature.

**Figure 1.** Schematic diagram of the reduction test device.

The reduction degree indicates the degree of difficulty of removing oxygen from iron oxides in the pellets. However, the oxides containing Mg, Si and Ca are barely be reduced under the experimental temperature and atmosphere conditions in this study. Therefore, the reduction degree (α) is generally treated as the mass percentage of oxygen removed from the iron oxides and is evaluated as:

$$\alpha = \frac{m_1 - m_t}{m_0} \quad (1)$$

where m_1 is the initial mass of pellets, (g), m_t is the mass of pellets after reduction time t , (g), m_0 is the total mass of oxygen theoretically capable of being removed, (g).

In the Equation (1), the total mass of removable oxygen in the pellets is evaluated assuming that all the oxygen of the combining iron exists in the form of Fe₂O₃; however, some Fe₃O₄ and FeO also occurred in the pellets. The degree of reduction should be calculated considering the mass loss in the experiment and the difference between the theoretical mass of oxygen and the actual weight of oxygen. In this study, the actual weight of oxygen was calculated assuming that Fe₂O₃, Fe₃O₄, and FeO exist in the pellets, and the reduction degree can be evaluated according to Equation (2).

$$\alpha = \frac{m_0 W_1 \times \frac{8}{71.85}}{m_0 W_2 \times \frac{48}{111.7}} \times 100 + \frac{m_1 - m_t}{m_0 \times \frac{W_2}{100} \times \frac{48}{111.7}} \times 100 \quad (2)$$

Equation (2) is simplified into the form of Equation (3)

$$\alpha = \left(\frac{0.111W_1}{0.430W_2} + \frac{m_1 - m_t}{m_0 \times 0.430W_2} \times 100 \right) \times 100 \quad (3)$$

where W_1 is the wustite (FeO) content before reduction, (%) and W_2 is the total iron (TFe) content before reduction, (%); 0.111 and 0.430 are necessary conversion.

The softening-melting experiment for different burden compositions was carried out in a melting-dripping furnace; the experimental apparatus is shown in Figure 2. The furnace was heated electrically using U-shape-Super Kanthal with a heating zone of about 600 mm in height and the maximum working temperature could reach 1600 °C. A $\Phi 75$ mm (inner diameter) graphite crucible with $\Phi 8$ mm dripping holes in its bottom was used in the experiments. The charging situation was assumed to be blast furnace loading, namely, 30 g dried that was 10–12.5 mm in diameter was placed on the bottom of the graphite crucible; then, 500 g sample (different burden composition) was put into a graphite crucible and formed a layer of burden; finally, the 90 g dried coke with a 10–12.5 mm diameter was tiled on the burden. After charging, the pressure bar and the charged crucible were placed in the melting-dripping tube, and ensure the thermocouple was wired well. To ensure pressure drop, it was necessary to seal the melting-dripping tube bottom well, preventing gas leaks.

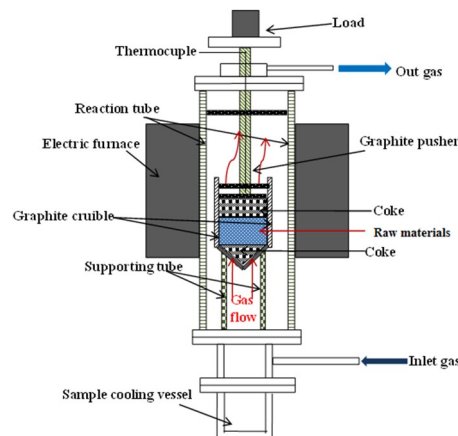


Figure 2. Experimental device for testing the melting property of iron-bearing materials.

The burden composition used in the tests is shown in Table 2. The PB and PC only used pellets, the MPB and MPC used a mixed burden (pellets + sinter). The softening-melting behavior of the four kinds of burden composition was investigated. In the four burden composition samples, the SiO₂ content in the pellets was increased from 4.63 to 5.18 wt%.

Table 2. Different burden composition used in the tests.

Sample	Pellets in Mixed Burden (%)	Sinters in Mixed Burden (%)
PB	100	0
PC	100	0
MPB	37	63
MPC	37	63

Softening-melting experiment conditions are depicted in Figure 3. After the temperature reached 1570 °C, the nitrogen gas was inserted quickly until ambient temperature to avoid oxidizing of reduced samples. A melting-dripping behavior and mechanism was achieved with an explicit index for the melting-dripping process, and the dripped and residual substance in the crucible were collected for further analysis.

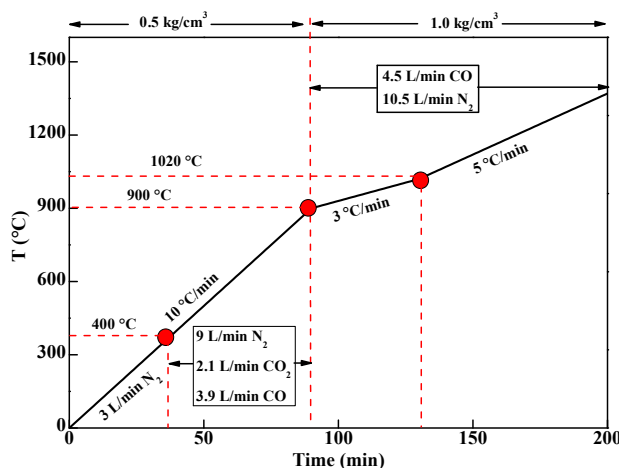


Figure 3. Experimental conditions for testing the melting properties.

3. Results

3.1. Effect of SiO₂ on the Characteristics of Pellets

3.1.1. Compressive Strength

Compressive strength indicates the ability of pellets to withstand a load during their storage and handling and the load of burden materials in a reduction furnace. The effect of SiO₂ content on the compressive strength of pellets is shown in Figure 4, which shows that the SiO₂ content has a negative relationship with the compressive strength of pellets. The compressive strength was 3.39 kN and 2.20 kN when the SiO₂ content were 2.19% and 8.13%, respectively. It could be observed that the compressive strength for all pellets meets the production requirements for blast furnaces, but the pellets with high SiO₂ content (5.18 wt% and 8.13 wt%) cannot meet the production requirements for shaft furnaces.

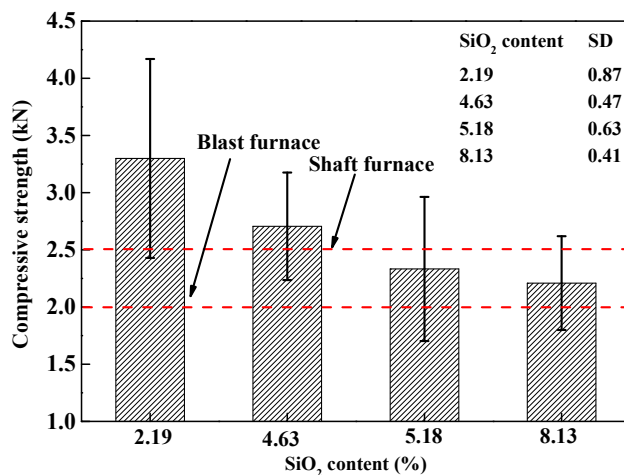


Figure 4. The effect of SiO₂ content on the compressive strength of pellets (average value of ten times).

3.1.2. Phase Composition

The phase compositions of pellets with different SiO₂ content were characterized by XRD. The results are shown in Figure 5. In the figure, it is revealed that phase compositions of pellets with 2.19 wt% was Fe₂O₃. As the SiO₂ content increased from 2.19 wt% to 8.13 wt%, the peaks corresponding to Fe₂O₃ weakened gradually. However, peaks related to SiO₂ were observed for the pellets with

8.13 wt%. No peaks corresponding to CaO, $2\text{FeO}\cdot\text{SiO}_2$, MgO, or Al_2O_3 were identified, meaning their concentrations were below the level detectable by XRD, which will be examined in a future study.

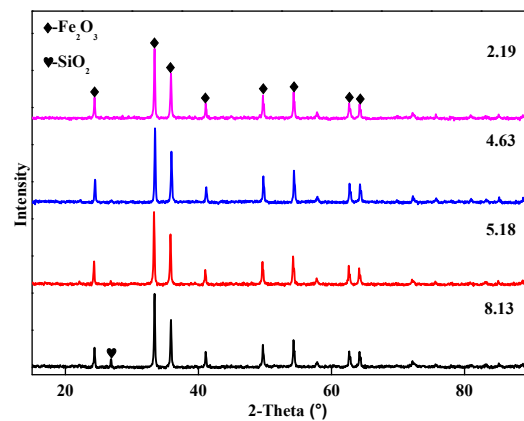


Figure 5. XRD analysis of pellets with different SiO_2 content.

3.1.3. Morphology Change

It is well-known that the microstructure of pellets is an important factor affecting its compressive strength. Figure 6 shows the microstructure of a polished cross-section of the pellets with different SiO_2 content. All the microstructures were taken at the similar magnifications in order to ensure that the grains distribution and size were captured. Figure 6 indicated the morphological features of the pellets with different SiO_2 content changed significantly. For the pellet with 2.19 wt% SiO_2 content (Figure 6a), the hematite existed in the form of euhedral crystalline, which appeared as a filamentous micro-crystal and had better recrystallization. The crystallite connected together compactly and distributed evenly. A small amount of silicate melts and pores occurred in the pellets.

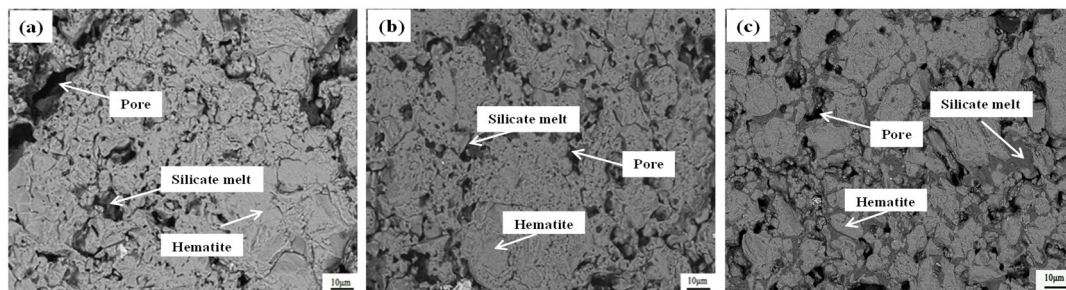


Figure 6. Microstructure of pellets with different SiO_2 contents: (a) 2.19, (b) 4.63 and (c) 8.13 wt%.

The pellets with 4.63 wt% SiO_2 (Figure 6b) had a semi-euhedral crystalline distribution across the surface. Compared to Figure 6a, a clear decrease in the euhedral crystalline was observed, the porous structure seemed to be starting to develop, and the silicate melt increased. The pellets with 8.13 wt% SiO_2 (Figure 6c) showed a further decrease of euhedral crystalline and more pores in the pellets. Some big pores were observed across the sample center and large amounts of silicate melt appeared in the core of the pellet. The pellets with high SiO_2 levels exhibited more pores, poor crystallization and more silicate melt. The results agreed well with the compressive strength presented in Figure 4. Thus, it could be concluded that the SiO_2 content changed the porosity and crystallization of the pellets, ultimately affecting their compressive strength.

3.2. Effect of SiO₂ on the Reduction Behavior of Pellets

3.2.1. Reduction Degree

Figure 7 shows the effect of SiO₂ content on the reduction degree of pellets under the constant reduction conditions. As shown in Figure 7, the reduction degree of pellets decreased with increasing SiO₂ content. The reduction degree was 75.22% and 46.19% for 2.19 wt% and 8.13 wt% SiO₂ contents in pellets, respectively. It was the similar reduction degree for 4.63 wt% and 5.18 wt% SiO₂ contents in pellets, which were 72.11% and 72.96%, respectively.

The reduction process of pellets occurs step by step in certain reduction conditions (Fe₂O₃→Fe₃O₄→FeO→Fe). Based on the XRD analysis in Section 3.2.2, the reduced FeO reacted with SiO₂ to generate 2FeO·SiO₂ (a substance with lower melting point and worse reductivity). According to the thermodynamic analysis as shown in Equation (4), 2FeO·SiO₂ generated easily above 900 °C. Therefore, the generated of 2FeO·SiO₂ inhibited the reduction behavior with increasing SiO₂ content in pellets.



In the reduction process, the pellets might undergo as following process: First, FeO content in pellets increased during the reduction process; Then, the FeO reacted with SiO₂ to generate 2FeO·SiO₂ (a substance with lower melting point and worse reductivity) and a little of liquid phase. Finally, the liquid phase inhabited the diffusion of reducing gas towards inside of pellets. Based on the process, the reduction degree decreased along with an increasing SiO₂ in pellets.

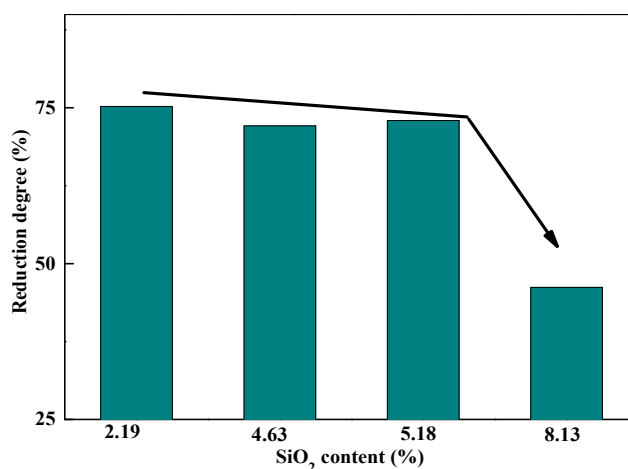


Figure 7. Effect of SiO₂ on the reduction degree of pellets.

3.2.2. Phase Compositions

The XRD patterns of reduced pellets with different SiO₂ content, reduced for 180 min under a constant atmosphere are shown in Figure 8. For the pellet with 2.19 wt% SiO₂ content, the main phases of reduced pellets were Fe and 2FeO·SiO₂. However, the diffraction peaks were detected belonged to SiO₂ for the pellets with 8.13 wt%. With increasing SiO₂ content in pellets, the diffraction peaks of 2FeO·SiO₂ strengthened gradually, whereas those of Fe weakened significantly, which is mainly attributed to the suppressed reduction behavior by the formation of 2FeO·SiO₂.

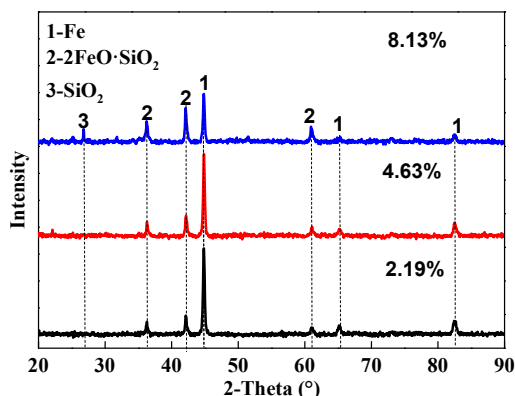


Figure 8. XRD analysis of reduction pellets with different SiO₂ content.

3.2.3. Morphology Change

Figure 9 shows the SEM images and EDS analysis of reduced pellets with different SiO₂ contents. The white area is metallic iron (point 3), the gray area is the wustite (point 1), and the black area is slag (point 2). The fayalite, which is a low melting point minerals, formed between wustite and metallic iron with increasing SiO₂ content in pellets during the reduction process.

It is easy to see that pellets with 2.19 wt% SiO₂ was reduced better than the pellets with 4.63 wt% and 8.13 wt%. The microstructure of the reduced pellet with 2.19 wt% SiO₂ showed that a uniform continuous area was formed. Further, the slag and wustite were surrounded by metallic iron, and SiO₂ did not appear in the pellets. With increasing SiO₂ content, it was observed that the wustite increased and metallic iron decreased, wustite reacted with SiO₂ to generate fayalite as shown in point 4 in Figure 9c. This tendency was more obvious and more fayalite formed for pellets with 8.13 wt% SiO₂. Based on the morphology analysis, the morphology structure change, resulting in the decrease of the reduction degree.

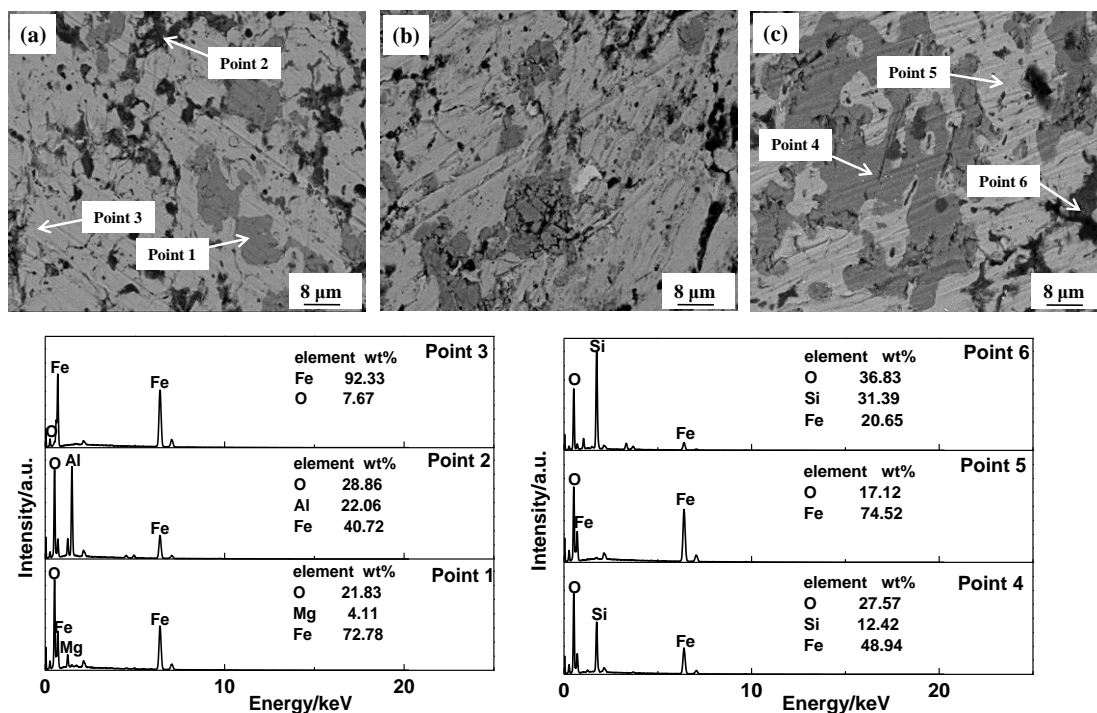


Figure 9. SEM images and EDS analyses of the reduced pellets with different SiO₂ content (a) 2.19, (b) 4.63, and (c) 8.13 wt%.

3.3. Effect of SiO₂ and Burden Composition on Melting Properties

3.3.1. Melting-Dripping Properties

The softening-melting behavior of iron-bearing materials plays an important role in the location, shape, and permeability of the cohesive zone, and blast furnace operations criteria also influence the cohesive zone. The melting start temperature (T_S) is usually defined as the temperature at which the pressure drop through the bed increases to 2 kPa; the dripping temperature (T_D) is defined as the temperature at which the first droplet of the melting materials drops to the crucible; and melting-dripping zone (T_D-T_S) reflects the thickness of the cohesive zone. Studying the softening-melting characteristics of different burden compositions help us to understand the formation of cohesive zones in the lower portion of blast furnace.

To investigate the effect of the burden compositions on the softening-melting characteristics of the burden, the main raw materials of PB and PC were used in this paper. The burden compositions are shown in Table 2, and the results are shown in Figure 10. In the case of using single pellets, the melting starting temperature (T_S) increased from 1162 °C to 1205 °C, the dripping temperature (T_D) increased from 1304 °C to 1338 °C, and the melting-dripping zone (T_D-T_S) decreased from 142 °C to 133 °C with increasing SiO₂ content from 4.63 wt% to 5.18 wt%. As the burden composition changed from MPB to MPC, T_S decreased from 1262 °C to 1241 °C, T_D decreased from 1385 °C to 1370 °C, and T_D-T_S was unchanged basically (about 120 °C). Meanwhile, the position distribution of the melting-dripping zone was determined with different burden compositions, as shown in Figure 11. The location of the melting-dripping zone moved down slightly and the melting-dripping zone became midthly narrower. Therefore, the melting behavior of the mixed burden was better, compared to the high SiO₂ content pellets.

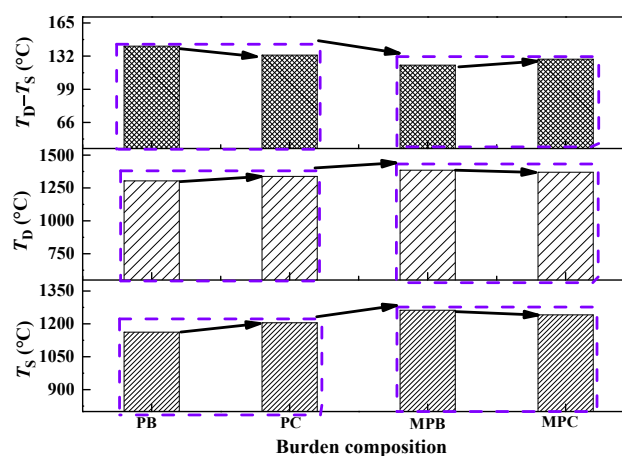


Figure 10. Effect of burden compositions of pellets on the melting behavior.

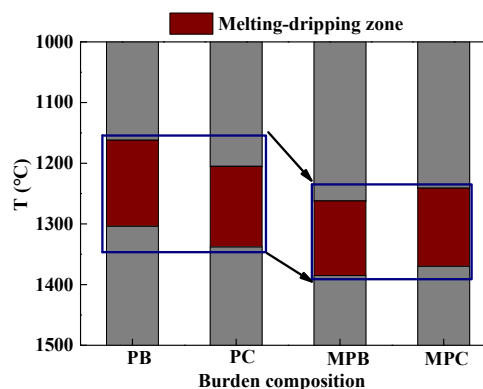


Figure 11. Effect of burden composition of pellets on the location of the cohesive zone.

3.3.2. The Permeability of Different Burden Compositions

To quantify the softening-melting behavior of the different burden compositions, the S-value was introduced. The S-value as a softening-melting characteristic value is to quantify the softening-melting behavior of the different burden compositions. A smaller S-value indicates a better permeability of the burden compositions. The S-value is calculated from the integral of the pressure drop function over the interval of melting temperature and dripping temperature, meaning the area below the pressure drop curve. The S-value is calculated by the following Equation (5):

$$S = \int_{T_S}^{T_D} (P_m - \Delta P_s) \cdot dT \quad (5)$$

where P_m is the pressure drop at certain temperature between $T_D - T_S$, and ΔP is the pressure drop at melting temperature T_S .

The effect of SiO_2 content in pellets and burden compositions on permeability is shown in Figure 12. With increasing SiO_2 content from 4.63 wt% to 5.18 wt%, the S-value increased from 1122.5 $\text{kP}\cdot^\circ\text{C}$ to 1526.1 $\text{kP}\cdot^\circ\text{C}$. The S-value of MPB and MPC were 605.6 $\text{kP}\cdot^\circ\text{C}$ and 1204.4 $\text{kP}\cdot^\circ\text{C}$, respectively. The results indicated that the higher SiO_2 content in pellets could deteriorate the permeability of BF, and adding some sinter with high basicity in the mixed burden could improve the permeability.

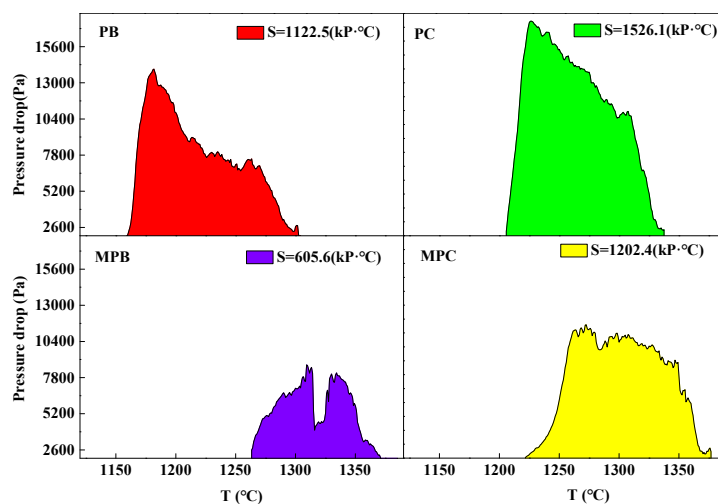


Figure 12. Effect of SiO_2 and burden composition on the permeability.

4. Discussion

4.1. Influence Mechanism of SiO_2 on Compressive Strength of Pellets

With increasing SiO_2 content in pellets, magnetite, which was obtained by non-oxidative magnetite or decomposed hematite, reacted with SiO_2 to form liquid phase at high temperatures. The FeO-SiO_2 binary phase diagram is shown in Figure 13. It could be seen that the liquidus temperature gradually decreased with increasing SiO_2 content from 0% to 23.5%. The liquidus temperature of 2FeO-SiO_2 (the red line in Figure 13) was only 1205 $^\circ\text{C}$. A large amounts of liquid phase (mainly 2FeO-SiO_2) formed, and then inhibited hematite crystallization during the oxidative roasting process. The crystallization capacity of 2FeO-SiO_2 was poor during the cooling process, which led to the formation of a glass phase. Therefore, the microstructure formed and resulted in the decrease of compressive strength of high SiO_2 pellets.

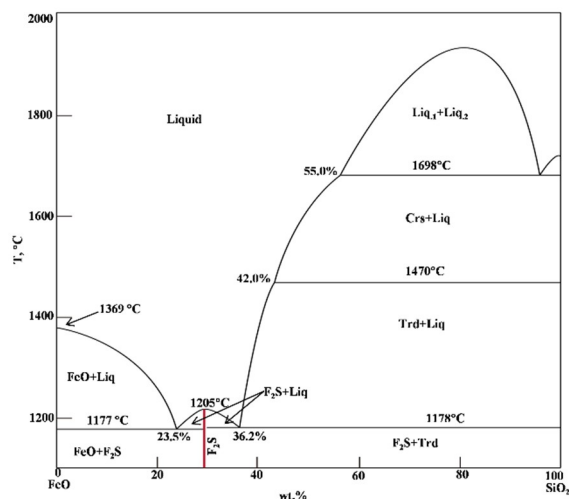


Figure 13. The binary phase diagram of FeO-SiO₂.

As illustrated in Figure 14, the solidification mechanism of the pellets can be concluded the liquid phases caused by the SiO₂ improve the consolidation of the pellets at low roasting temperatures, while the liquid phases of low melting point increases with increasing roasting temperature and SiO₂ content. The excessive amount of liquid phase shrinks at the cooling process and forms many small cracks in the pellets, which causes the decrease of compressive strength of high SiO₂ content pellets. In addition, the excessive liquid phase inhibits the direct contact between the solid particles, and resulting in poor crystallization, more primary crystal and more glass phases. In conclusion, the roasting temperature and heating rate should be strictly controlled in the pellet roasting process during the production of acid pellets to prevent the generation of an excessive liquid phase and too much temperature fluctuation.

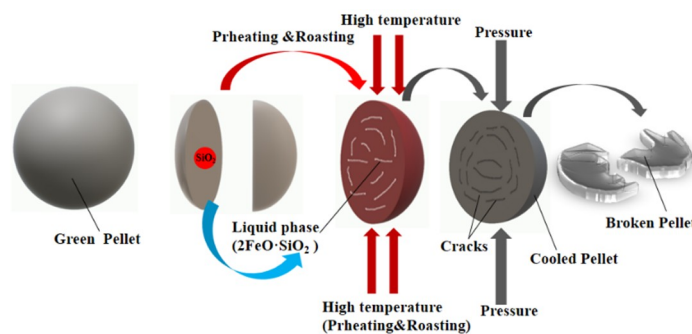


Figure 14. Schematic diagram of the liquid phase formation in the pellets and its effects.

In order to understand the effect of SiO₂ on the liquid phase amount, the sample of the CaO-Fe₂O₃-SiO₂ system with different SiO₂ content was roasted by using chemical reagents and results are shown in Figure 15. It could be seen that the main phase of minerals was hematite and liquid phase where the gray part was hematite, and the black part was a liquid phase, as shown in Figure 15. The liquid phase gradually increased, hematite decreased with increasing SiO₂ content. For lower SiO₂ content, the liquid phase was separated the hematite, and the shape was irregular. The liquid phase gradually integrated into a whole, and the shape was more regular with as the SiO₂ content increased.

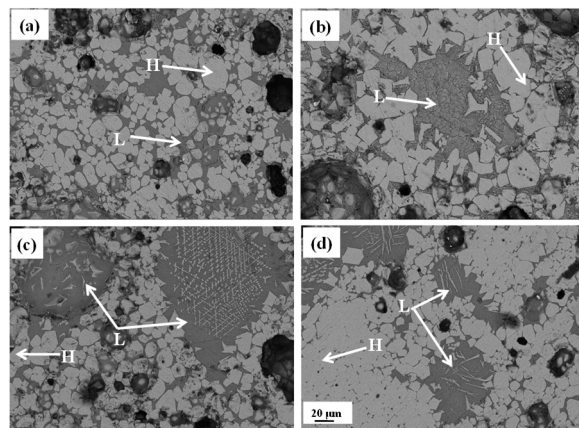


Figure 15. The effect of SiO₂ on liquid phase when SiO₂ is (a) 4%, (b) 6%, (c) 8%, and (d) 10%. L: Liquid phase; H: Hematite.

The minerals compositions of the samples for different SiO₂ contents are shown in Figure 16. Hematite was 65.09% with 4% SiO₂ addition. However, the hematite content sharply decreased with the increasing SiO₂ content: 61.59%, 49.68%, and 41.56% for the SiO₂ contents of 6%, 8% and 10%, respectively. The liquid phase was 34.9%, 38.41%, 50.32% and 58.44% for the SiO₂ additions of 4%, 6%, 8%, and 10%, respectively. With increasing SiO₂ content, the liquid phase sharply increased, resulting in a decrease of compressive strength.

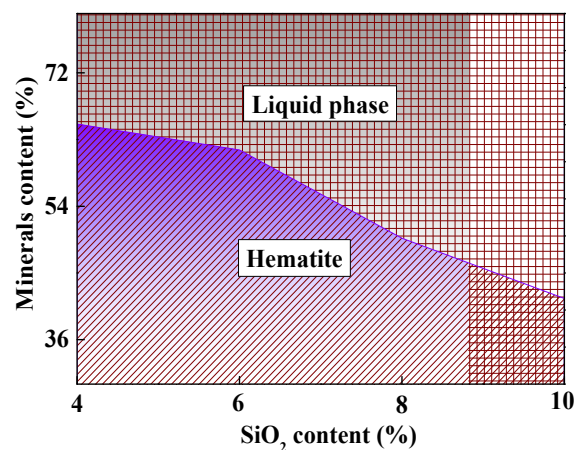


Figure 16. The minerals contents of different SiO₂ sample.

4.2. Effect of Burden Compositions on Melting Start Temperature

In order to further understand the effect of burden composition on melting start temperature, the chemical compositions of different burden composition at melting start temperature are provided in Table 3. The main components were wustite and metallic iron, and only a small amount of Fe₂O₃ for all samples. In the case of using mixed burden, the greater CaO content in the sinter resulted in more CaO at T₅. The reducibility of mixed burden is better than that of the single pellet, mainly because CaO reacted with Fe₂O₃ and formed calcium ferrite.

Different chemical compositions caused different melting start temperatures: the mixed burden contained more metallic iron and other high-melting point materials (such as MgO and Al₂O₃), resulting in the increase of melting start.

Table 3. The chemical compositions of the sample at the melting start temperature (wt%).

Sample	FeO	TFe	CaO	SiO ₂	Al ₂ O ₃	MgO	MFe
PB	57.54	75.88	1.00	6.33	0.27	0.50	23.24
PC	60.34	77.80	0.74	5.64	0.37	0.57	22.93
MPB	49.00	69.75	7.43	6.92	2.05	1.34	29.19
MPC	51.28	76.55	7.19	5.46	1.95	1.42	28.45

X-ray diffraction analysis of the samples interrupted at T_S are shown in Figure 17. The major phases were FeO, $2\text{FeO}\cdot\text{SiO}_2$, $\text{Ca}_2\text{Mg}(\text{Si}_2\text{O}_7)$, and Fe. With increasing SiO_2 content in pellets from 4.63 wt% to 5.18 wt%, the FeO increased gradually and metallic iron decreased. No peaks corresponding to akermanite could be identified. However, peaks related to $2\text{FeO}\cdot\text{SiO}_2$ were observed, which were attributed to the reaction of FeO and SiO_2 , as shown in Equation (4).

In the case of using mixed burden, the intensity of the diffraction peaks of FeO and Fe were further enhanced, whereas the $2\text{FeO}\cdot\text{SiO}_2$ phase did not change significantly and the $\text{Ca}_2\text{Mg}(\text{Si}_2\text{O}_7)$ phase appeared. This indicated that the FeO, Fe, and $\text{Ca}_2\text{Mg}(\text{Si}_2\text{O}_7)$ increased, but $2\text{FeO}\cdot\text{SiO}_2$ decreased. Based on the XRD analysis, the main slag phase of the pellets alone is $2\text{FeO}\cdot\text{SiO}_2$, which is a low melting point phase (1150 °C); however, the main slag phase of mixed burden is akermanite, which is a high melting point phase. The different slag phase can cause the change of the melting start temperature.

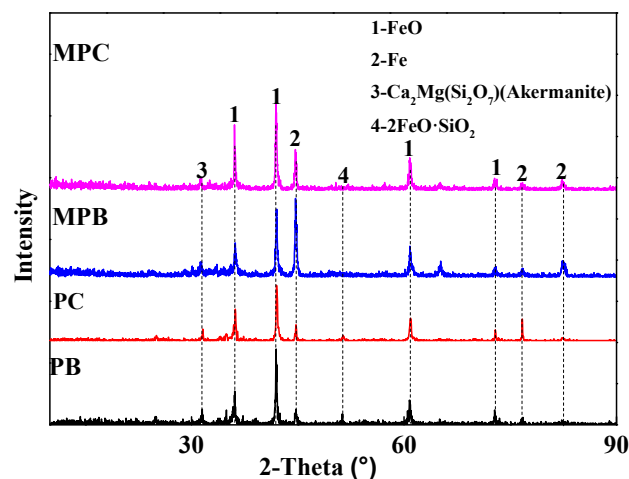
**Figure 17.** The XRD analysis of different burden composition in the melting temperature.

Figure 18 shows the microscopic morphology of samples at T_S . The figure shown that the main phases were metallic iron phase (white), wustite phase (gray) and slag phase (black) for all sample. For PB (Figure 18a), the main phase was wustite and a small account of metallic iron, indicated that the PB had poor reducibility at T_S . The shape of the wustite and metallic iron was regular and round, and there were a few slag phases between the wustite. The main elements of the slag were Fe, Si, and O as shown in point 3, so the slag phase of the PB was the iron silicate series at T_S .

For MPB (Figure 18b), the metallic iron increased significantly and fluidity of the slag phase improved. The wustite and metallic iron phase changed into irregular shape, and connected to each other. Compared with MB, the slag content increased, and the compositions mainly were include Ca, O and a small amount Fe and Si. These components caused the increase of melting point of the slag, and the reducibility of mixed burden improved, which led to the increase of T_S .

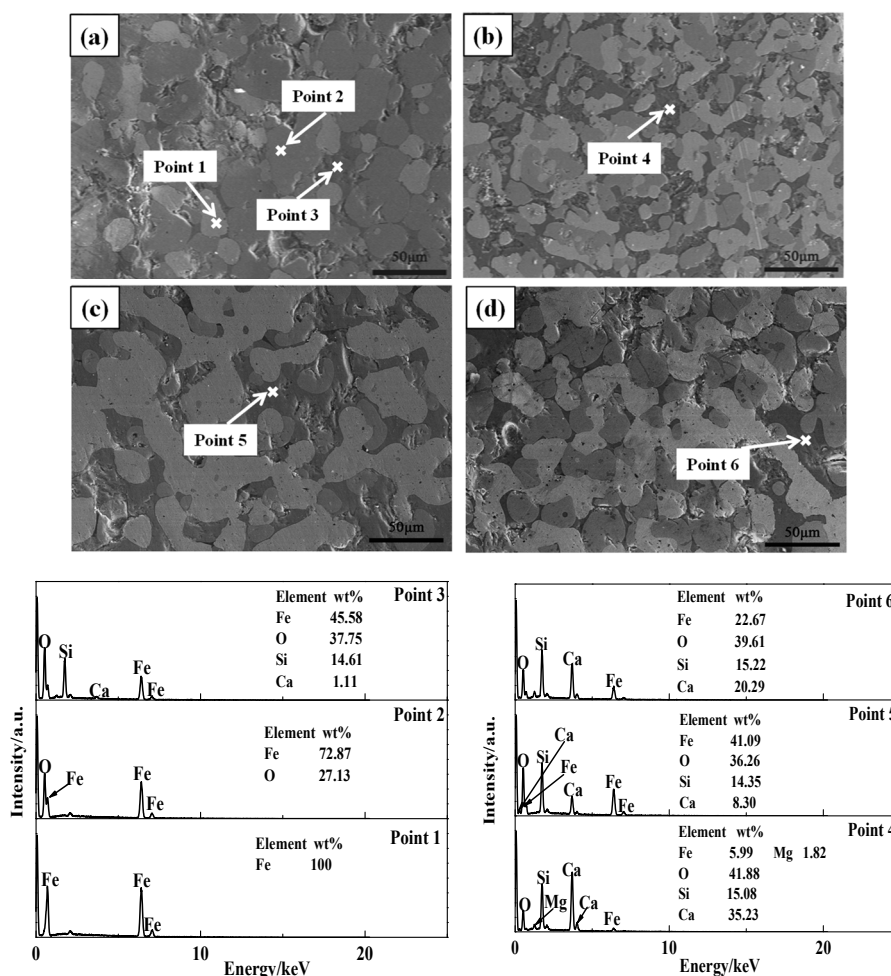


Figure 18. SEM images and EDS analysis of polished pellets at melting temperature with different burden composition: (a) PB (b) MPB, (c) PC, (d) MPC.

For PC, the main phase was metallic iron, slag phase and a small amount of wustite with increasing SiO_2 content in the pellets. The metallic iron was connected into a larger sheet shape, and there was a small amount of wustite along its edge. The slag phase amount increased significantly, but the basic composition was consistent with PB, that is, iron silicate. The more metallic iron caused the increase of T_S . For MPC, metallic iron and wustite were the main components at T_S , the slag phase was only a small part, but the main components of the slag phase were similar to MPB.

To clearly understand the element distribution of different burden compositions, the EDS maps of the elements distribution, including Fe, O, Si, Ca, and Mg taken from the PB and MPB images at the melting start temperature are shown in Figures 19 and 20. The main elements of PB were Fe, Si, O, and some Ca, where Si existed in wustite and did not appear in metallic iron as shown in Figure 19. However, the main elements of MPB were Fe, Ca, Mg, Si, and O, in which the Si existed in the slag. SiO_2 existed as the FeO-SiO_2 solution (formed 2FeO-SiO_2) in PB, whereas it mainly appeared as akermanite (high melting point) in the MPB slag phase.

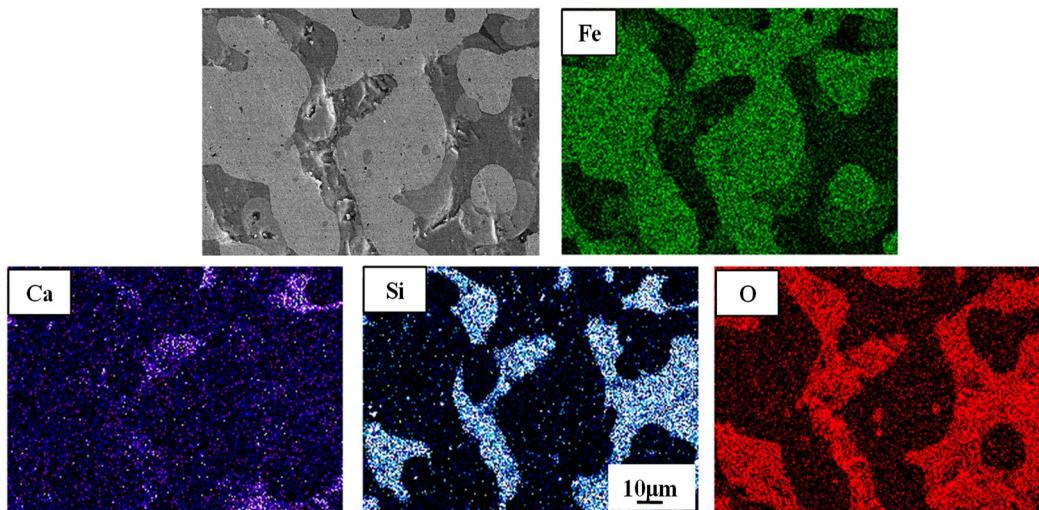


Figure 19. Element distributions of PB at T_5 .

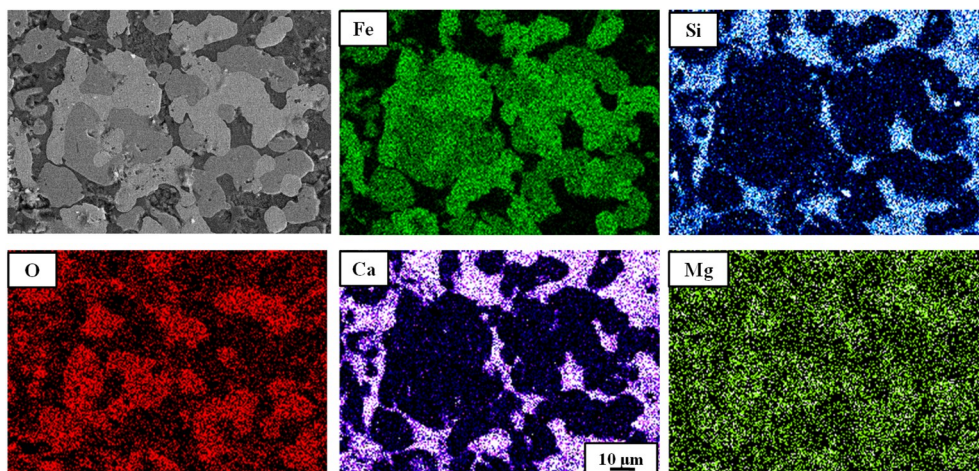


Figure 20. Element distributions of MPB at T_5 .

4.3. Dripping Behavior of Different Burden Composition

To better understand the mechanism by which SiO_2 content in the pellets affects the dripping behavior of the burden composition, the dripping slag was analyzed by X-ray diffraction and chemical compositions. The X-ray diffraction results for the dripping slag are shown in Figure 21. For the pellet alone, the main phases of PB were hedenbergite magnesian ($\text{Al}_{0.14}\text{Ca}_{0.92}\text{Fe}_{0.41}\text{Mg}_{0.53}\text{O}_6\text{Si}_2$), magnesium iron calcium silicate ($\text{Ca}_{0.043}\text{Fe}_{0.802}\text{Mg}_{1.155}\text{O}_6\text{Si}_2$), and magnesium iron oxide (MgFe_2O_4); With increasing SiO_2 in the pellets, the amount of hedenbergite magnesian increased, the diffraction peaks were detected belonged to AlFeO_3 , MgSiO_3 , and MgAl_2O_4 . For the mixed burden, the main phases of MPB were olivine ($\text{Fe}_{0.59}\text{Mg}_{1.41}\text{O}_4\text{Si}$) and sekaninaite ($\text{Mg}_{0.34}\text{Fe}_{1.66}\text{Al}_4\text{Si}_5\text{O}_8$). Compared with MPB, the diffraction peaks of olivine and sekaninaite strengthened gradually for MPC, which was mainly attributed to the reduction behavior being suppressed by the formation of FeSiO_4 . The different melting points for the slag could indicate different dripping behaviors.

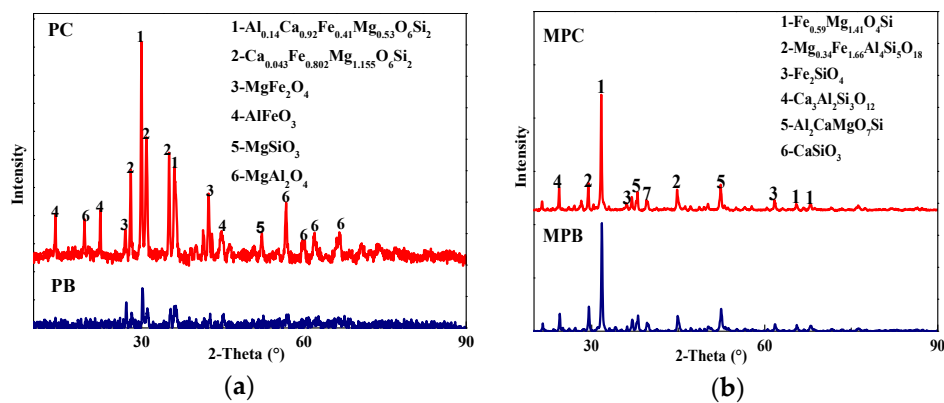


Figure 21. XRD pattern of dripping products for pellets alone and mixed burden: (a) pellets alone; (b) mixed burden.

The chemical compositions of the dripping slag are shown in Table 4. The SiO_2 content of pellets alone insignificantly changed and the reduction behavior decreased with increasing SiO_2 . Compared with the pellets alone, the reduction behavior of mixed burden was better and SiO_2 content decreased. The MgO content decreased, while the CaO and Al_2O_3 contents increased with increasing SiO_2 content in the mixed burden.

Table 4. Chemical composition of the dripping slag (wt%).

Sample	TFe	FeO	MgO	SiO_2	CaO	Al_2O_3
PB	16.23	18.83	4.11	56.88	10.06	7.85
PC	22.33	20.11	3.36	55.36	8.01	4.24
MPB	13.66	17.67	8.23	29.08	32.38	11.04
MPC	11.40	14.09	6.58	32.15	33.02	14.03

5. Conclusions

- (1) When the SiO_2 content in pellets increased from 2.19% to 8.13%, the compressive strength decreased from 3.39 kN to 2.20 kN, because more silicate melts formed by the reaction between SiO_2 and wustite. These silicate melts inhibited the contact between the solid Fe_2O_3 particles and resulted in the poor recrystallization of Fe_2O_3 in pellets.
- (2) The reduction degree decreased with increasing SiO_2 contents in pellets. When the SiO_2 content in pellets increased from 2.19% to 8.13%, the reduction degree decreased from 75.22% to 46.19%. The main reasons were as follows: First, FeO content in pellets increased during the reduction process; Then, the FeO reacted with SiO_2 to generate $2\text{FeO}\cdot\text{SiO}_2$ (a substance with lower melting point and worse reductivity) and a little of liquid phase. Finally, the liquid phase inhibited the diffusion of reducing gas towards the inside of pellets.
- (3) Increasing the SiO_2 content had negative effects on the melting-dripping properties of pellets. The melting-dripping properties can be improved by adding some sinter with high basicity in the mixed burden, because more akermanite (higher melting point) formed in the mixed burden during the reduction and melting process.

Author Contributions: H.G. and X.J. contributed to the material synthesis, performed the experiments, material characterization, and data analysis, and wrote the paper; F.S. and X.Z. revised the paper and refined the language; Q.G. and H.Z. contributed to the design of the experiment.

Funding: The financial supports of National Science Foundation of China (NSFC 51874080, NSFC 51774071, NSFC 51604069) and the Fundamental Research Funds for the Central Universities, China (N182504008) are much appreciated.

Acknowledgments: The authors wish to acknowledge the contributions of associates and colleagues in Northeastern University of China.

Conflicts of Interest: The authors declare no conflict of interest.

References

1. Friel, J.J.; Erickson, E.S. Chemistry, Microstructure, and Reduction Characteristics of Dolomite-Fluxed Magnetite Pellets. *Metall. Mater. Trans. B* **1980**, *11*, 233–243. [[CrossRef](#)]
2. Pal, J.; Ghoral, S.; Agarwal, S.; Nandi, B.; Chakraborty, T.; Das, G.; Prakash, S. Effect of Blaine Fineness on the Quality of Hematite Iron Ore Pellets for Blast Furnace. *Miner. Process Extr. Metall. Rev.* **2014**, *36*, 83–91. [[CrossRef](#)]
3. Gao, Q.J.; Shen, F.M.; Wei, G.; Jiang, X.; Zheng, H.Y. Effects of MgO Containing Additive on Low-Temperature Metallurgical Properties of Oxidized Pellet. *J. Iron Steel Res. Int.* **2013**, *20*, 25–28. [[CrossRef](#)]
4. Tang, J.; Chu, M.S.; Xue, X.X. Optimized use of MgO flux in the agglomeration of high-chromium vanadium-titanium magnetite. *Int. J. Miner. Metall. Mater.* **2015**, *22*, 371–380. [[CrossRef](#)]
5. Gao, Z.X.; Cheng, G.J.; Xue, X.X.; Yang, H.; Duan, P.N. Property Investigations of Low-Grade Vanadium-Titanium Magnetite Pellets with Different MgO Contents. *Steel Res. Int.* **2018**, *89*, 1700543. [[CrossRef](#)]
6. Long, H.M.; Li, J.X.; Wang, P.; Shi, S.Q. Reduction kinetics of carbon containing pellets made from metallurgical dust. *Ironmak. Steelmak.* **2012**, *39*, 585–592. [[CrossRef](#)]
7. Guo, Y.H.; Xie, J.; Gao, J.J.; Xu, H.J.; Qie, J.M. Study on the Production and Metallurgical Properties of Fluxed Pellets with High Hematite Content. *Metallurgist* **2017**, *61*, 638–645.
8. Iljana, M.; Kempainen, A.; Paananen, T.; Mattila, O.; Pisila, E.; Kondrakov, M.; Fabritius, T. Effect of adding limestone on the metallurgical properties of iron ore pellets. *Int. J. Miner. Process.* **2015**, *141*, 34–43. [[CrossRef](#)]
9. Umadevi, T.; Kumar, P.; Lobo, N.F.; Prabhu, M.; Mahapatra, P.C.; Ranjan, M. Influence of Pellet Basicity (CaO/SiO₂) on Iron Ore Pellet Properties and Microstructure. *ISIJ Int.* **2011**, *51*, 14–20. [[CrossRef](#)]
10. Qing, G.; Wu, K.; Tian, Y.; An, G.; Yuan, X.; Xu, D.; Huang, W. Effect of the firing temperature and the added MgO on the reduction swelling index of the pellet with low SiO₂ content. *Ironmak. Steelmak.* **2018**, *45*, 83–89. [[CrossRef](#)]
11. Wang, H.T.; Sohn, H.Y. Effects of Reducing Gas on Swelling and Iron Whisker Formation during the Reduction of Iron Oxide Compact. *Steel Res. Int.* **2012**, *83*, 903–909. [[CrossRef](#)]
12. Umadevi, T.; Kumar, A.; Karthik, P.; Srinidhi, R.; Manjini, S. Characterisation studies on swelling behaviour of iron ore pellets. *Ironmak. Steelmak.* **2018**, *45*, 157–165. [[CrossRef](#)]
13. Dwarapudi, S.; Ghosh, T.K.; Shankar, A.; Tathavadkar, V.; Bhattacharjee, D.; Venugopal, R. Effect of pellet basicity and MgO content on the quality and microstructure of hematite pellets. *Int. J. Miner. Process.* **2011**, *99*, 43–53. [[CrossRef](#)]
14. Dwarapudi, S.; Devi, T.U.; Rao, S.M.; Ranjan, M. Influence of pellet size on quality and microstructure of iron ore pellets. *ISIJ Int.* **2008**, *48*, 768–776. [[CrossRef](#)]
15. Mohanty, M.K.; Mishra, S.; Mishra, B.; Sarkar, S. Effect of Basicity on the Reduction Behavior of Iron Ore Pellets. *Arab. J. Sci. Eng.* **2018**, *43*, 5989–5998. [[CrossRef](#)]
16. Shen, F.M.; Gao, Q.J.; Jiang, X.; Wei, G.; Zheng, H.Y. Effect of magnesia on the compressive strength of pellets. *Int. J. Miner. Metall. Mater.* **2014**, *21*, 431–437. [[CrossRef](#)]
17. Zhang, J.L.; Wang, Z.Y.; Xing, X.D.; Liu, Z.J. Effect of aluminum oxide on the compressive strength of pellets. *Int. J. Miner. Metall. Mater.* **2014**, *21*, 339–344. [[CrossRef](#)]
18. Wang, S.; Guo, Y.F.; Yang, L.; Fu, G.H.; Zheng, F.Q.; Chen, F.; Yang, L.Z.; Jiang, T. Investigation of solidification mechanism of fluorine-bearing magnetite concentrate pellets. *Powder Technol.* **2018**, *332*, 188–196. [[CrossRef](#)]
19. Guo, H.W.; Bai, J.L.; Zhang, J.L.; Li, H.G. Mechanism of Strength Improvement of Magnetite Pellet by Adding Boron-bearing Iron Concentrate. *J. Iron Steel Res. Int.* **2014**, *21*, 9–15. [[CrossRef](#)]
20. Chen, J.W.; Chen, W.B.; Mi, L.; Jiao, Y.; Wang, X.D. Kinetic Studies on Gas-Based Reduction of Vanadium Titano-Magnetite Pellet. *Metals* **2019**, *9*, 95. [[CrossRef](#)]

21. Wang, G.; Wang, J.S.; Xue, Q.G. Kinetics of the Volume Shrinkage of a Magnetite/Carbon Composite Pellet during Solid-State Carbothermic Reduction. *Metals* **2018**, *8*, 1050. [[CrossRef](#)]
22. Gao, Q.J.; Jiang, X.; Zheng, H.Y.; Shen, F.M. Induration Process of MgO Flux Pellet. *Minerals* **2018**, *8*, 389. [[CrossRef](#)]



© 2019 by the authors. Licensee MDPI, Basel, Switzerland. This article is an open access article distributed under the terms and conditions of the Creative Commons Attribution (CC BY) license (<http://creativecommons.org/licenses/by/4.0/>).